International Journal of Nanoelectronics and Materials
Volume 13 (Special Issue) Dec 2020 (249-258)

First-Principles Study of CH_4 and NH_3 Adsorption on Graphene Oxide Epoxy and Graphene Oxide Hydroxyl

MSM Shukri[1,2], MNS Saimin[1,2], MH Samat[2], N Abdullah[3], SZN Demon[3*], NA Halim[3,4] and MFM Taib[1,2]

[1]*Faculty of Applied Sciences, Universiti Teknologi MARA, 40450 Shah Alam, Malaysia.*
[2]*Ionic Materials and Devices (iMADE), Institute of Science, Universiti Teknologi MARA, 40450 Shah Alam, Malaysia.*
[3]*Centre for Defence Foundation Studies, National Defence University of Malaysia, 57000 Kuala Lumpur, Malaysia.*
[4]*Research Centre for Chemical Defence, National Defence University of Malaysia 57000 Kuala Lumpur, Malaysia.*

ABSTRACT

Chemical functionalities of graphene oxide play an important part in anchoring gas molecules and perhaps selective mechanism in gas sensor. The adsorption behavior of methane (CH_4) and ammonia (NH_3) gas molecules on graphene oxide epoxy (GO-epoxy) and graphene oxide hydroxyl (GO-hydroxyl) were investigated using first-principles calculations within density functional theory (DFT) method. The structural properties (bond length and adsorption distance), electronic properties (band structures and density of states), adsorption energy (E_{ads}) and Mulliken charge transfer were calculated using generalized gradient approximation of Perdew-Burke-Ernzerhof (GGA-PBE) as implemented in DMol³ and Cambridge Serial Total Energy Package (CASTEP) computer codes. After geometrical optimization, there are slight differences in structural properties and electronic properties before and after adsorption of CH_4 and NH_3 on GO-epoxy and GO-hydroxyl. In comparison between CH_4 and NH_3 on GO-epoxy and GO-hydroxyl, highest adsorption energy was calculated for NH_3 adsorbed on GO-hydroxyl (E_{ads} = -0.775 eV) indicated higher chance of charge transfer to occur compared to others structures. The overall result shows that physisorption behavior is the main interaction between CH_3 and NH_4 on GO-epoxy and GO-hydroxyl for gas sensors based on GO.

Keywords: Graphene Oxide (GO), Methane, Ammonia, First-Principles Study, Density Functional Theory (DFT).

1. INTRODUCTION

First introduced in 2004 by Geim et al. [1], graphene among various other carbonaceous materials emerges as the center of attention amongst researchers. Graphene, shaped like honeycomb structures, has attracted much attention due to its superior properties such as high specific surface area, high electrical and thermal conductivity, good mechanical strength and intriguing transport properties [2, 3]. For these reasons, graphene has been used in various applications such as in air separation, natural gas separation, chemical separation, battery, sensor, wastewater treatment, CO_2 capture and storage, and many more [4, 5]. In gas detection particularly, every carbon atom in monolayer graphene becomes surface atom available for gas adsorption giving higher capability of detection. Graphene oxide (GO) and reduced graphene oxide (rGO) have another advantage compared to monolayer defect-free graphene. The presence of dangling oxygen functional groups on their surface and edges provide sensitive and selective detection toward several organic compounds [5].

*Correspoding Author: *zulaikha@upnm.edu.my*

Surface adsorption affected the electron transport through graphene as adsorbed molecules will bring changes to electronic structure of graphene. Graphene based sensors has been reported to detect hydrogen (H_2), nitrogen monoxide (NO), nitrogen dioxide (NO_2), methane (CH_4), ammonia (NH_3), carbon monoxide (CO) and carbon dioxide (CO_2) gas molecules [6–8]. CH_4 is highly valuable as an energy source for domestic and industrial applications but can be regarded as toxic gas to the environment [8]. NH_3 is produced in many industrial processes and from natural decomposition of organic matter [9]. Reliable detection of CH_4, NH_3 and other toxic gases can be used for monitoring air pollution in the atmosphere and protecting the environment [10, 11].

Defect free or pristine graphene can exhibit remarkable electronic properties in its 2D electronic band structure but this high-quality graphene cannot be produced in large scale without being too costly [4, 5, 12]. On the other hand, GO and rGO can be produced using cheaper chemical method such as Hummer's method. Furthermore, the oxygen functional groups on the surface or edge of graphene prevent bundling of graphene during device processing [13, 14]. Although the exact structures of GO are still a subject to debate due to its nonstoichiometry [15], it is widely accepted that the primary oxidation functional groups are epoxy (C (C-O-C)) and hydroxyl (-OH) groups on the basal plane of GO with some carboxyl (-COOH) and carbonyl (C=O) groups at the edges of graphene as introduced from the well-known Lerf-Klinowski model [16, 17].

Understanding the interaction between gas molecules and surface of GO is the key to develop better gas sensor. There is various adsorption mechanism such as chemisorption, physisorption and charge transfer that can attributed to the change of electronic structure in graphene. In gas sensor experiment done by Zöpfl et al, NO_2 gas was found to give opposite response of H_2 and CH_4 upon adsorption on rGO surface indicated selective sensing toward particular gas [18]. The decrease of resistance in rGO sensor is due to charge transfer effect by NO_2. Another gas sensing experiment using NO_2 and NH_3 had produced similar decrease in GO's resistance upon adsorption even though the gasses induced different type of charge carriers in graphene [19]. Although many experimental studies were performed to show practical use of graphene-based sensor, computational studies at molecular level can provide more detailed information to elucidate mechanism between adsorbed gas molecules and graphene surface [11, 20-25]. The knowledge from theoretical studies can give insight to better design of graphene-based gas sensor.

In this work, first-principles calculations were performed to investigate the structural properties, electronic properties, adsorption energy and Mulliken charge transfer of CH_4 and NH_3 adsorption on graphene with an epoxy-functional group (GO-epoxy) and graphene with hydroxyl-functional group (GO-hydroxyl).

2. METHODOLOGY

All the first-principles calculations in this work were performed based on the density functional theory (DFT) method using DMol^3 and Cambridge Serial Total Energy Package (CASTEP) modules in Materials Studio software. The electron exchange-correlation interactions were expressed with a generalized gradient approximation (GGA) in the form of the Perdew-Burke-Ernzerhof (PBE) functional [26]. The GGA-PBE functional has been successfully used to describe the interaction between organic molecules and a carbon-based substrate or an inorganic substrate. The orbital cut-off for the plane-wave basis expansion is chosen to be 7.0 Å. During relaxations, the position of all atoms was allowed to fully relax until the force on each atom is less than 0.02 eV/Å between two iconic steps and the convergence of the electronic self-consistent energy is less than 10-4 eV. Integration over the Brillouin zone was performed by using the Gamma-centered Monkhorst-Pack scheme [27] with 5×5×1 *k*-points, together with

Gaussian smearing broadening of 0.01 Ha. The double numerical plus polarization (DNP) was selected and the DFT semi-core pseudopotential (DSPP) was applied for core treatment. The total system is modeled using a 4×4 graphene supercell with a vacuum spacing of 15 Å, including graphene with oxygen functional group and with the adsorption of CH_4 and NH_3 gas molecules. The geometrical optimization was performed using fixed distance from CH_4 and NH_3 molecules to GO which is 2.5 Å. As a preliminary test, we have optimized the atomic geometry of 4×4 graphene supercell using the aforementioned calculation methods and parameters. After full relaxation, the lattice constant is 2.46 Å, which is in good agreement with the experimental value [28]. The atomic geometries of the CH_4 and NH_3 gas molecules were also optimized. The calculated bond lengths for CH_4 and NH_3 are 1.097 Å and 1.022 Å, respectively.

3. RESULT AND DISCUSSION

3.1 Structural and Electronic Properties

Graphene oxide (GO) is assumed to consist of either epoxy, hydroxyl, carboxyl or carbonyl. Throughout this paper, epoxy and hydroxyl groups were introduced to the pristine graphene structure by placing the O and OH species within a carbon. The geometry of GO with one epoxy group (GO-epoxy) and GO with one hydroxyl group (GO-hydroxyl) were investigated as a substrate for CH_4 and NH_3 adsorption as illustrated in Fig. 1 (a) and (b). The epoxy-functional group adsorbs with O preferentially on the bridge of carbon atoms [29]. Previous report showed that the O atom was most stable at the C-C bridge site of the graphene [30]. The hydroxyl functional group adsorbs with O preferentially on top of C atoms and pointing in the direction towards the center of a 6-fold ring. The orientation of CH_4 and NH_3 molecules were arranged by placing the molecules on top of each functional group (epoxy and hydroxyl) with the H tripod of CH_4 directed away from the functional groups (Fig. 1(c) and (d)) and hydrogen tripod of NH_3 directed towards the functional groups (Fig. 1(e) and (f)).

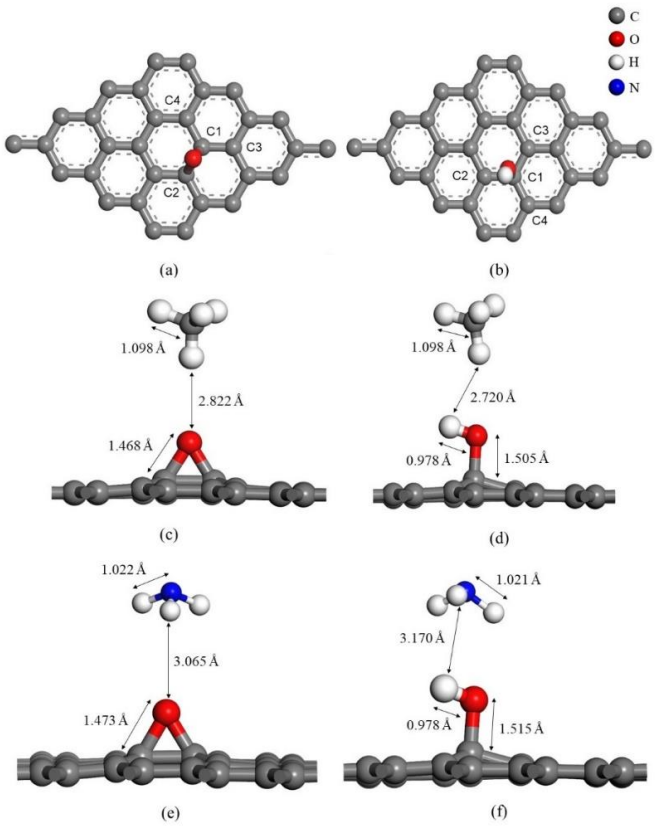

Figure 1. Optimized structures of (a) GO-epoxy, (b) GO-hydroxyl, (c) CH_4 on GO-epoxy and (d) CH_4 on GO-hydroxyl, (e) NH_3 on GO-epoxy and (f) NH_3 on GO-hydroxyl.

The structural properties of GO-epoxy, GO-hydroxyl and both CH_3 and NH_4 gases on each GO substrate are listed in Table 1. After geometrical optimization, the graphene plane shows slight distortion because of the destruction of sp^2 hybridization of carbon atoms binding with functional groups, with epoxy functional group shows the most elongation of C-C bond length (1.517 Å) for C1-C2 bond length at O atom compare to C1-C2 bond length of hydroxyl functional group (1.502 Å) at O and H atoms. This elongation of C-C bond length compare to ideal C-C bond length (1.42 Å) [28, 31] suggests that the conjugation degree of GO sheets decreases. The local curvature from this geometric property enhances the local reactivity and it is expected that this can play an important role in gas adsorption [32]. The obtained bond lengths of the GO-epoxy and GO-hydroxyl (C-C, C-O and O-H) are in agreement with other previous reports [33, 34] thus, conforming our modelled geometry. After adsorption with CH_4, not much difference in bond length occurred except for the C-O bond length that slightly increased after adsorption. On the other hand, the C-C bond length significantly reduced after NH_3 adsorption while the C-O bond length increased.

Table 1 The optimized bond lengths and adsorption distance, *d* (defined as the distance of nearest atoms between GO and CH_4/NH_3) of GO-epoxide, GO-hydroxyl, CH_4 on GO-epoxy, CH_4 on GO-hydroxyl, NH_3 on GO-epoxy and NH_3 on GO-hydroxyl

Structures	C1-C2 (Å)	C1-C3 (Å)	C1-C4 (Å)	C-O (Å)	O-H (Å)	C-H (Å)	N-H (Å)	*d* (Å)
GO-epoxy	1.517	1.468	1.467	1.464	-	-	-	-
	1.5197[a]	1.4723[a]	1.4695[a]	1.466[b]	-	-	-	-
CH_4 on GO-epoxy	1.510	1.468	1.468	1.468	-	1.098	-	2.822
NH_3 on GO-epoxy	1.504	1.462	1.462	1.473	-	-	1.022	3.065
GO-hydroxyl	1.502	1.502	1.500	1.498	0.977	-	-	-
	1.5064[a]	1.5069[a]	1.5064[a]	1.514[b]	0.981[b]	-	-	-
CH_4 on GO-hydroxyl	1.501	1.501	1.501	1.505	0.978	1.098	-	2.720
NH_3 on GO-hydroxyl	1.496	1.495	1.495	1.515	0.978	-	1.021	3.170

[a] Ref. [35]
[b] Ref. [36]

For the CH_4 on GO-epoxy, the distance between CH_4 and the epoxy group anchored on GO is 2.822 Å. For the CH_4 on GO-hydroxyl, the distance between CH_4 and the hydroxyl group anchored on GO is 2.720 Å. CH_4 tends to form hydrogen bonding with the hydrogen atom in the hydroxyl group. Comparing these two values, it suggests that CH_4 is much closer to GO-hydroxyl compared to GO-epoxy after geometrical optimization. However, for NH_3 on GO-epoxy and GO-hydroxyl, the nearest distance of the atoms between NH_3 and functional groups are longer than CH_4 on functional groups which are 3.065 Å and 3.170 Å, respectively. The obtained values of *d* in the range of 2.72–3.17 Å are within reasonable distances for physisorption [34].

The band structure describes the ranges of energy that an electron within the solid may have (allowed bands) and ranges of energy that an electron may not have (band gaps or forbidden gaps). The band structures of GO-epoxy and GO-hydroxyl along with the high symmetry direction of Brillouin zone at G-F-Q-Z-G are displayed in Fig. 2. The results show the direct type of band gap at F-Q point with 1.604 eV and 1.215 eV gaps for GO-epoxy and GO-hydroxyl, respectively. These gaps are higher than pristine graphene (0 eV) [37]. The reasons behind the gap opening can be due to the breakdown of the sublattice symmetry in graphene by the OH group and change in carbon hybridization from sp^2 to sp^3 due to strong covalent bonding between C and O atoms [33]. The band structures after CH_4 and NH_3 adsorption on GO are presented in Fig. 3. After CH_4 adsorption, the conduction band shifts to the lower energy region

which increases the intensity near the Fermi level. This leads to the decreasing of band gap to 1.593 eV and 1.214 eV which are not much different before the adsorption of CH_4. The band gaps of NH_3 on both GO are slightly higher than CH_4 on GO. For NH_3 on GO-hydroxyl, the band gap is increased to 1.232 eV due to the reduction of C-C bond length after adsorption. It is calculated that the band gap changes in GO-epoxy as a result of interactions with CH_4 and NH_3 are 0.69% and 0.44%, respectively. While, the band gap changes in GO-hydroxyl after CH_4 and NH_3 interactions are 0.08% and 1.40%, respectively. These changes in GO by adsorption of CH_4 and NH_3 molecules suggest it is possible for GO to detect both CH_4 and NH_3 molecules.

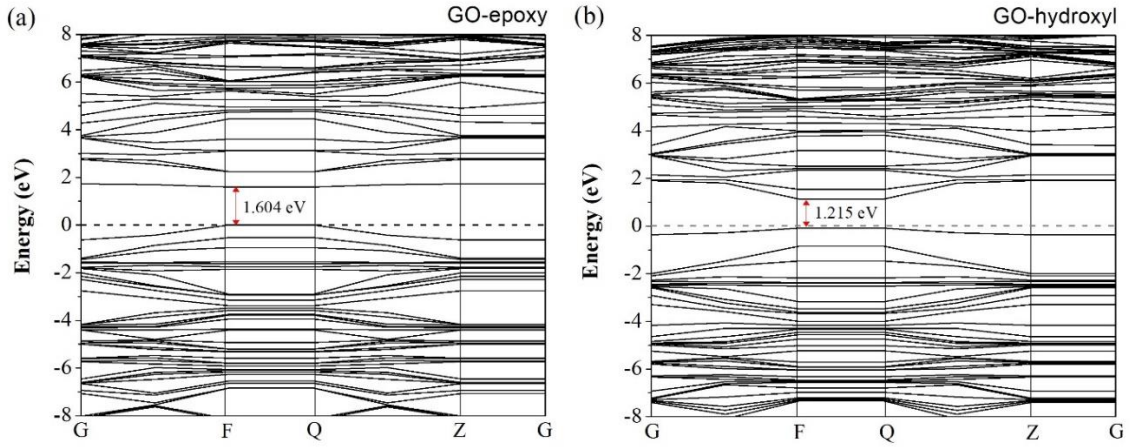

Figure 2. Band structures of (a) GO-epoxy and (b) GO-hydroxyl.

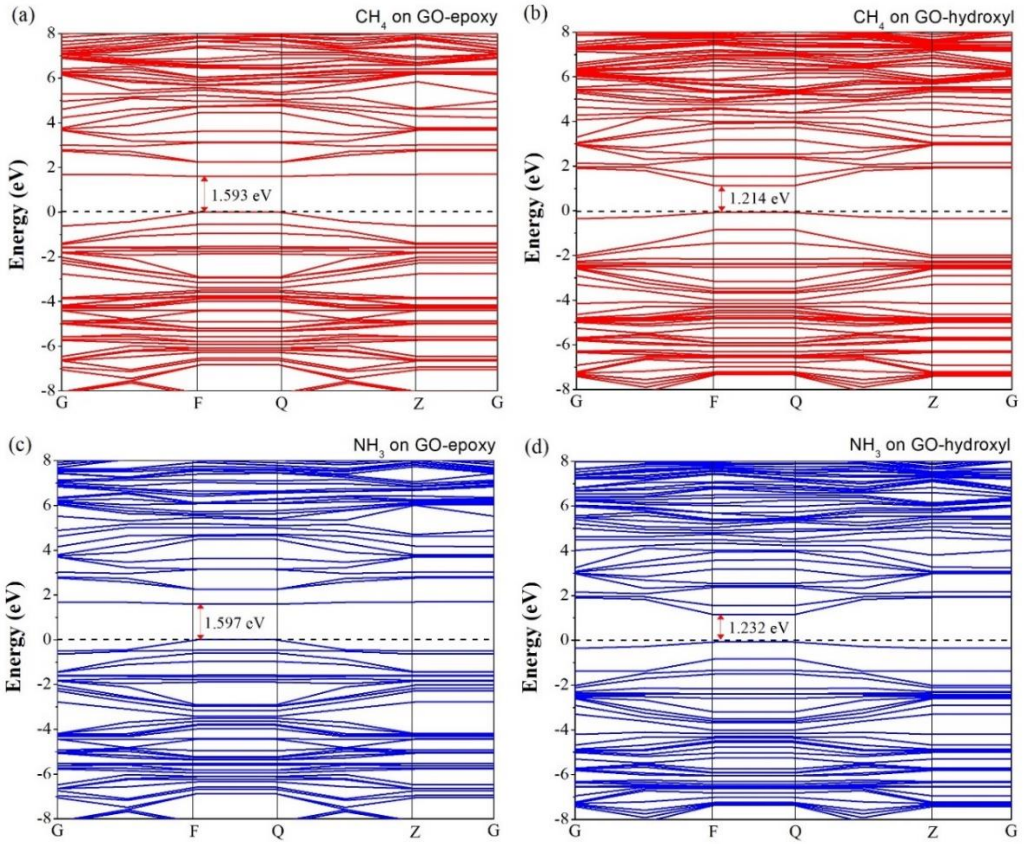

Figure 3. Band structures of (a) CH_4 on GO-epoxy, (b) CH_4 on GO-hydroxyl, (c) NH_3 on GO-epoxy and (d) NH_3 on GO-hydroxyl.

The total density of states (DOS) of GO-epoxy and GO-hydroxyl, as well as CH_4 and NH_3 on both GO, are shown in Fig. 4. There is not much difference between the presented DOS between each structure. It can be seen that the density of electrons near the Fermi level (0 eV) is very low. Weak bonding between the gaseous and GO is another characteristic of physisorption. The peaks around -4 eV for CH_4 on GO and -6 eV for NH_3 on GO are slightly increased which are due to the presence of CH_4 and NH_3 on GO-epoxy and GO-hydroxyl. For more details on the DOS results, the partial density of states (PDOS) for each atom in GO-epoxy and GO-hydroxyl are presented in Fig. 5 while the PDOS of CH_4 and NH_3 on both GO are presented in Fig. 6. The states of all atoms around the Fermi level mainly come from *p* orbitals. The PDOS for C and O atoms shows the high contribution of O *2p* states at the valence band. On the other hand, more C *2p* can be seen at the conduction band compare to O *2p*. For GO-hydroxyl, we can see the presence of H states from the hydroxyl functional groups which contains the H atom. After CH_3 and NH_4 adsorption on GO, no obvious change occurs except the presence of states nearby valence band edge above the Fermi level changes the value of band gaps. Also, the new H states coming from CH_4 appear at -4 eV and H states from NH_3 appears at -6 eV which are far from the Fermi level.

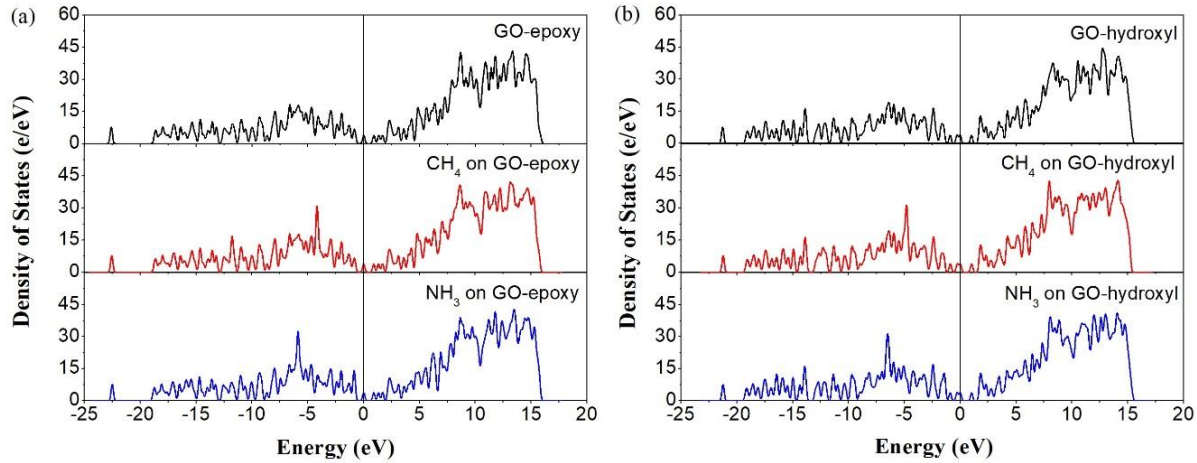

Figure 4. Total density of states (DOS) of (a) GO-epoxy, CH_4 on GO-epoxy and NH_3 on GO-hydroxyl and (b) GO-hydroxyl, CH_4 on GO-hydroxyl and NH_3 on GO-hydroxyl.

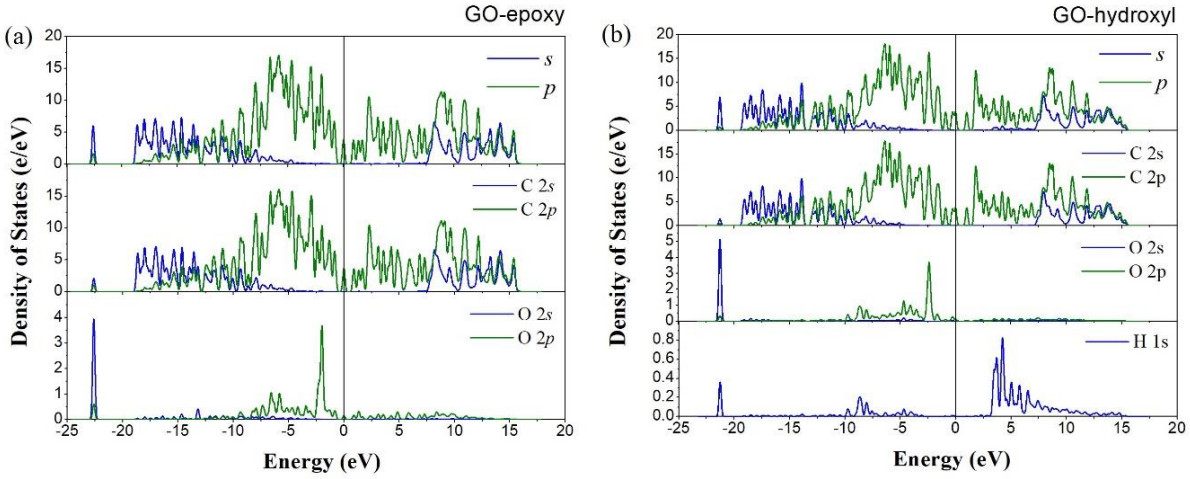

Figure 5. Partial density of states (PDOS) of (a) GO-epoxy and (b) GO-hydroxyl.

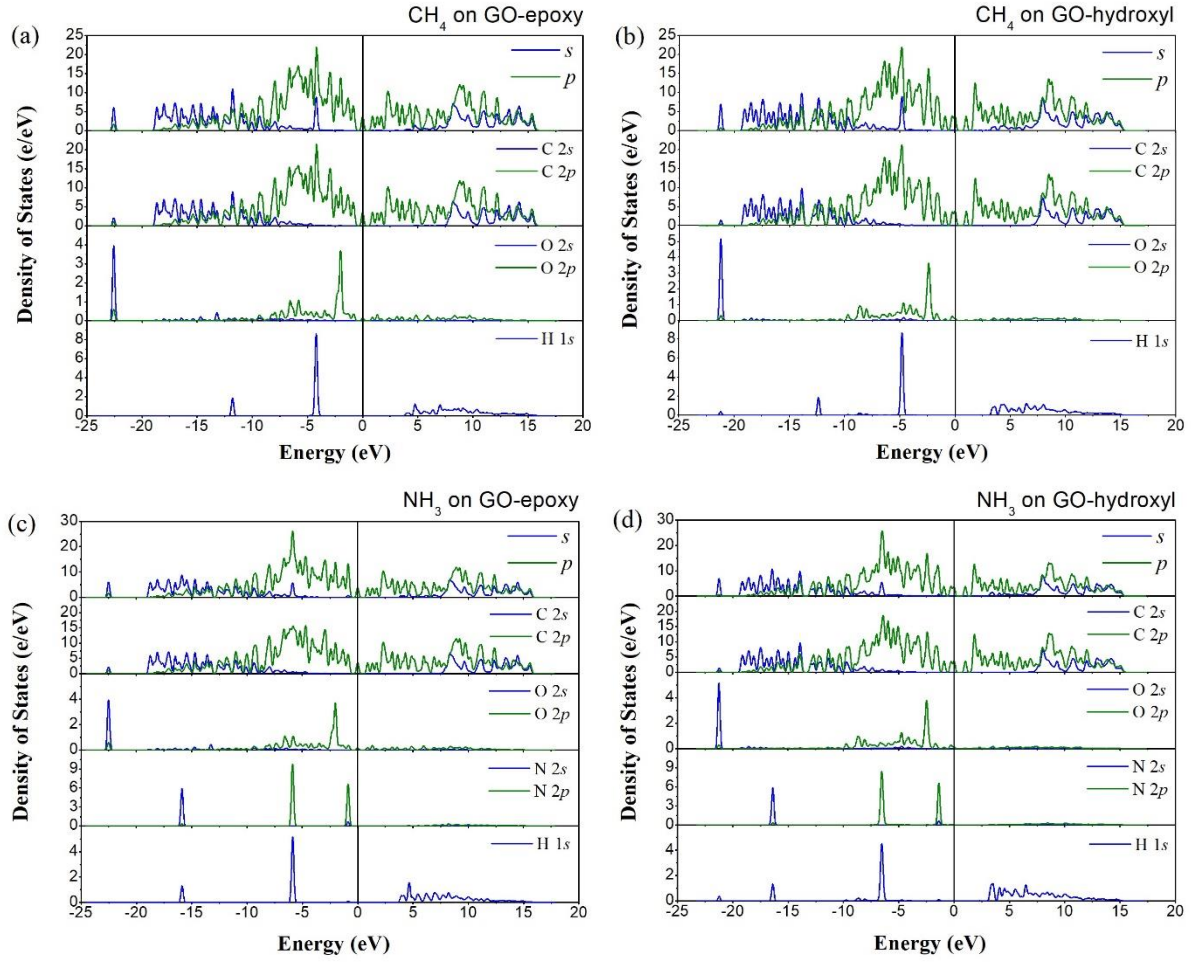

Figure 6. Partial density of states (PDOS) of (a) CH_4 on GO-epoxy (b) CH_4 on GO-hydroxyl (c) NH_3 on GO-epoxy and (d) NH_3 on GO-hydroxyl.

3.2 Adsorption Energies and Charge Analysis

In order to investigate the adsorption probability on GO-epoxy and GO-hydroxyl surface, the adsorption energies, E_{ads} are calculated according to the following equation:

$$E_{ads} = E_{total}(GO + CH_4/NH_3) - E_{substrate}(GO) - E_{gas}(CH_4/NH_3) \quad (1)$$

From the above equation, E_{total} represents the energy of the entire system, $E_{substrate}$ is the energy of the substrate system alone and E_{gas} corresponds to the energy of the isolate gas molecule. The lower adsorption energy values indicate greater stability.

The calculated E_{ads} for CH_4 and NH_3 adsorbed on respective GO surface are shown in Table 2. CH_4 was adsorbed vertically onto the O atom of the epoxy group in the GO-epoxy substrate. The adsorption energy for this configuration was -0.590 eV. On the other, CH_4 was adsorbed vertically atop the H atom of the hydroxyl group in the GO-hydroxyl substrate and the adsorption energy for this configuration was -0.451 eV. The O atom in the GO-epoxy is believed to cause a doping effect and subsequently enhanced the adsorption energy of CH_4 which explains more negative adsorption energy compared to GO-hydroxyl [38]. Though hydroxyl functional groups also facilitate the adsorption through H bonding, the presence of the epoxy group provides an active site for CH_4 adsorption. Furthermore, research by Kim et al. [39] using DFT with GGA-PW91 functional showed that the epoxy groups are much more stable compared

to hydroxyl groups in graphene, which validates our results. The adsorption energy of NH_3 on GO-hydroxyl was found to be stronger than NH_3 on GO-epoxy. Other finding also presented there is higher probability of NH_3 adsorption on the hydroxyl group compare to the adsorption on the epoxy group [40]. The adsorption preference for CH_4 and NH_3 is contributed by the magnitude of electronic changes occurred in GO after adsorption. From the bandgap analysis, the percentage of bandgap change is higher for CH_4/GO-epoxy and NH_3/GO-hydroxyl. The preference may imply higher sensitivity to particular gas type. Overall, the small value of adsorption energies indicates CH_3 and NH_4 on GO undergo physisorption.

Charge transfer (ΔQ) of CH_4 and NH_3 on GO-epoxy and GO-hydroxyl are also calculated based on the Mulliken population analysis as shown in Table 2. The charge transfer between the gases and GO during the adsorption process are very poor. The sign of the ΔQ indicates donor or acceptor properties. A positive ΔQ means some electrons transferred from molecules to the surfaces. Charge population analysis of CH_4 on GO-epoxy shows that there are 0.003 e charge transfers from CH_4 molecule to the GO-epoxy, suggesting that GO-epoxy behaves as a donor and CH_4 as an acceptor. This indicates that GO-epoxy loss electrons and CH_4 gained electrons. Otherwise, for another system, the gas molecules behave as a donor which transfers electrons to the GO. This is consistent with other reports for NH_3 on graphene where small charge transfer from NH_3 to the graphene surface has occurred [41]. For NH_3 on GO-hydroxyl, there is a slightly stronger charge transfer from NH_3 to GO-hydroxyl compare to NH_3 on GO-epoxy.

Table 2 Adsorption energy (E_{ads}) and charge transfer ΔQ of CH_4 and NH_3 on GO-epoxy and GO-hydroxyl

Structure	E_{ads} (eV)	ΔQ (e)
CH_4 on GO-epoxy	-0.590	+0.003
CH_4 on GO-hydroxyl	-0.451	-0.002
NH_3 on GO-epoxy	-0.529	-0.001
NH_3 on GO-hydroxyl	-0.775	-0.004

4. CONCLUSION

In summary, the structural properties, electronic properties, adsorption energies and charge transfer of CH_4 and NH_3 adsorption on GO-epoxy and GO-hydroxyl were investigated using the first-principles study based on DFT method. The adsorption of CH_4 and NH_3 on GO-epoxy and GO-hydroxyl alter the structural and electronic properties of GO. It can be concluded that the adsorption of CH_4 on GO-epoxy was found to be stronger than the adsorption of CH_4 on GO-hydroxyl. However, for adsorption of CH_4 and NH_3 on GO-hydroxyl, GO-hydroxyl shows a preference for NH_3 over CH_4. There is only a small contribution of charge transfer occurred between the GO and the gas molecules. These findings could provide an understanding on adsorption behavior of CH_4 and NH_3 on GO-epoxy and GO-hydroxyl.

ACKNOWLEDGEMENTS

The authors gratefully acknowledge support from Chemical Defence Research Centre UPNM (CHEMDEF) for research grant (UPNM/2018/CHEMDEF/ST/3). The authors would also like to thank Ministry of Education, Malaysia and the government of Malaysia for the allocated research funding (ISIS-NEWTON/2019/SG/01).

REFERENCES

[1] Geim, A. K., Novoselov, K. S., Nat. Mater. **6**, 3 (2007) 183–191.
[2] Sun, Y., Wu, Q., Shi, G., Graphene based new energy materials. Energy Environ. Sci. **4**, 4 (2011) 1113–1132.
[3] Stankovich, S., Dikin, D. A., Dommett, G. H. B., Kohlhaas, K. M., Zimney, E. J., Stach, E. A., Piner R. D., Nguyen, S. T., Ruoff, R. S. Nature **442** (2006) 282–286.
[4] Coroş, M., Pogăcean, F., Măgeruşan, L., Socaci, C., Pruneanu, S., Front. Mater. Sci. **13**, 1 (2019) 23–32.
[5] Demon, S. Z. N. , Kamisan, A. I., Abdullah, N., Noor, S. A. M., Ong, K. K., Kasim, N. A. M., Yahya, M. Z. A., Manaf, N. A. A., Azmi, A. F. M., Halim, N. A., Sens. and Mater. **32,** 2 (2020) 759–777.
[6] Tian, W., Liu, X., Yu, W., Appl. Sci. **8**, 7 (2018) 1118.
[7] Schedin, F., Geim, A. K., Morozov, S. V., Hill, E. W., Blake, P., Katsnelson, M. I., Novoselov, K. S., Nat. Mater. **6**, 9 (2007) 652–655.
[8] Assar, M., Karimzadeh, R., J. Colloid Interface Sci. **483**, 2 (2016) 275–280.
[9] Zhang, L., Tan, Q., Kou, H., Wu, D., Zhang, W., Xiong, J., Sci. Rep. **9**, 1 (2019) 1–10.
[10] Wu, D., Peng, Q., Wu, S., Wang, G., Deng, L., Tai, H., Wang, L., Yang, Y., Dong, L., Zhao, Y., Zhao, J., Sun, D., Lin, L., Sensors **18**, 12 (2018) 4405.
[11] Ehab, S., Ahmad, I. A., Phys. Lett. A **384**, 29 (2020) 126775.
[12] Theng, L. L., Yahya, I., Mohamed, M. A., Taib, M. F. M., "First Principle Study of Graphene-Carbon Nanotubes Hybrid (GCH) Structure for Advanced Nanoelectronics Devices," in 2018 IEEE International Conference on Semiconductor Electronics (ICSE), (2018) 250–253.
[13] Patel, K. D., Singh, R. K., Kim, H. W., Mater. Horizons, **6**, 3 (2019) 434–469.
[14] Aliyev, E., Filiz, V., Khan, M. M., Lee, Y. J., Abetz, C., Abetz, V., Nanomaterials **9**, 8 (2019) 1180.
[15] Mao, S., Pu, H., Chen, J. RSC Adv. **2**, 7 (2012) 2643–2662.
[16] Manna, B., Raha, H., Chakrabarti, I., Guha, P. K., IEEE Trans. Electron. Devices **65**, 11 (2018) 1–8.
[17] Lerf, A., He, H., Forster, M., Klinowski, J., J. Phys. Chem. B **102**, 23 (1998) 4477–4482.
[18] Zöpfl, A., Lemberger, M., König, M., Ruhl, G., Matysika, F., Hirsch, T., Faraday Discuss. **173** (2014) 403-414.
[19] Fowler, J. D., Allen, M. J., Tung, V. C., Yang, Y., Kaner, R. B., Weiller, B. H., ACS Nano **3**, 2 (2009) 301–306.
[20] Leenaerts, O., Partoens, B., Peeters, F. M., Microelectronics J. **40**, 4–5 (2009) 860–862.
[21] Lazar, P., Karlický, F., Jurečka, P., Kocman, M., Otyepková, E., Šafářová, K., Otyepka, M., J. Am. Chem. Soc. **135,** 16 (2013) 6372–6377.
[22] Zhou, M., Lu, Y-H., Cai, Y-Q., Zhang, C., Feng, Y-P., Nanotechnology **22**, 28 (2011) 385502.
[23] Ma, L., Zhang, J-M., Xu, K-W., Ji, V., Appl. Surf. Sci. **343** (2015) 121–127.
[24] Liu, X-Y., Zhang, J-M., Xu, K-W., Ji, V., Appl. Surf. Sci **313** (2014) 405–410.
[25] Gao, X., Zhou, Q., Wang, J., Xu, L., Zeng, W., Nanomaterials **10** (2020) 299.
[26] Perdew, J. P., Burke, K., Ernzerhof, M., Phys. Rev. Lett. **77**, 18 (1996) 3865–3868.
[27] Monkhorst, H. J., Pack, J. D., Phys. Rev. B **16**, 4 (1977) 1748–1749.
[28] Gray, D., McCaughan, A., Mookerji, B., "Crystal Structure of Graphite, Graphene and Silicon," in Lecture Cambridge: Massachusetts Institute of Technology, (2009).
[29] Esrafili, M. D., Dinparast, L., J. Phys. Chem. Solids **117** (2018) 42–48.
[30] Li, Y., Pathak, B., Nisar, J., Qian, Z., Ahuja, R., EPL (Europhysics Lett) **103**, 2 (2013) 28007.
[31] Fan, Y., Xiang, Y., Shen, H., Research **2020** (2020) 5618021.
[32] Lee, Y., Lee, S., Hwang, Y., Chung, Y-C., Appl. Surf. Sci. **289**, 2 (2014) 445–449.
[33] Yan, J. A., Chou, M. Y., Phys. Rev. B – Condens. Matter. Mater. Phys. **82**, 12 (2010) 21–24.
[34] Kuisma, E., Hansson, C. F., Lindberg, T. B., Gillberg, C. A., Idh, S., Schröder, E., J. Chem. Phys. **144**, 18 (2016) 184704.
[35] Yao, J. H., Yin, Z. L., Li, Y. W., IOP Conf. Ser. Earth Environ. Sci. **81** (2017) 012026.

[36] Song, C., Wang, J., Meng, Z., Hu, F., Jian, X., Chem. Phys. Chem. **19**, 13 (2018) 1579–1583.
[37] Shukri, M. S. M., Saimin, M. N. S., Yaakob, M. K., Yahya, M. Z. A., Taib, M. F. M., Appl. Surf. Sci. **494** (2019) 817–828.
[38] Moon, H. S., Lee, J. H., Kwon, S., Kim, I. T., Lee, S. G., Carbon. Lett. **16**, 2 (2015) 116–120.
[39] Kim, M. C., Hwang, G. S., Ruoff, R. S., J. Chem. Phys. **131**, 6 (2009) 1–6.
[40] Peng, Y., Li, J., Front. Environ. Sci. Eng. **7**, 3(2013) 403–411.
[41] Leenaerts, O., Partoens, B., Peeters, F. M., Phy. Rev. B – Condens. Matter Mater. Phys. **77**, 12 (2008) 1–6.